Geoderma 287 (2017) 90–97

Contents lists available at ScienceDirect

Geoderma

journal homepage: www.elsevier.com/locate/geoderma

Evaluation of TrueCell program for estimating point capillary pressure — saturation parameters for Flint sand

S. Clark Cropper [a,*], Edmund Perfect [b], Chu-Lin Cheng [c], Larry McKay [b], Misun Kang [d]

[a] Math and Science Division, Volunteer State Community College, Gallatin, TN 37066, USA
[b] Department of Earth and Planetary Sciences, University of Tennessee – Knoxville, Knoxville, TN 37996, USA
[c] School of Earth, Environmental, and Marine Sciences, Department of Civil Engineering, University of Texas-Rio Grande Valley, Edinburg, TX 78539, USA
[d] Department of Earth and Planetary Sciences, University of California – Davis, Davis, CA 95616, USA

ARTICLE INFO

Article history:
Received 17 September 2016
Accepted 26 September 2016

Keywords:
Capillary pressure-saturation functions
Inverse estimation
Neutron radiography
Point hydraulic parameters
Soil water retention
TrueCell

ABSTRACT

The purpose of this paper is to compare inverse estimates of point capillary pressure–effective saturation, $S_e(\psi)$, parameters and functions with independently measured $S_e(\psi)$ parameters and functions. Average capillary pressure–effective saturation functions, $<S_e>(\psi)$, were measured for Flint sand using a hanging water column setup and 9 packed columns, with heights varying between 4.3 cm and 55.0 cm. TrueCell, a Fortran program, was employed to inversely estimate point $S_e(\psi)$ parameters and functions from the $<S_e>(\psi)$ data sets. The TrueCell estimates were then compared with point $S_e(\psi)$ parameters and functions determined by neutron radiographic imaging of a single hanging water column setup. One sample t-tests indicated that there were no significant differences (at $p < 0.05$) between the mean values of the inversely estimated point parameters and the corresponding neutron imaging values. However, the individual TrueCell predictions produced variable results compared to the measured point parameter set. Relatively few parameter estimates fell within the 95% confidence intervals of the neutron imaging estimates, and some deviations were quite large. These deviations were related to subtle variations in column packing, rather than differences in column height. Although this study has produced support for inverse modeling with TrueCell, it is important to note that individual predictions of $S_e(\psi)$ parameters and functions were often at odds with the independent measurements. Thus, TrueCell should be used with caution. In future studies of a similar nature, it would be desirable to independently determine point parameters and functions on multiple columns, rather than on a single column as was done here. Additionally, future research might want to examine the relationship between variations among individual parameters within a parameter set and the resulting predicted function.

1. Introduction

The capillary pressure–saturation function is a key hydraulic property used to characterize water retention in the vadose zone and to facilitate the prediction of relative permeability. Parameters describing this function are used as model inputs to numerically simulate a variety of critical hydrologic issues related to the environment (e.g., permafrost thawing due to climate change, fate and transport of contaminants in the vadose zone) and energy resources (e.g., oil and gas recovery, geologic carbon sequestration in confined brine aquifers).

The capillary pressure–saturation function is frequently determined experimentally in the laboratory by measuring outflow from a sample of finite height as it is subjected to a series of step changes in capillary pressure using a hanging water column, pressure cell, or centrifuge. Changes in average saturation within the sample are determined from the outflow measurements. Parameters for input into numerical models are then obtained by fitting a mathematical expression, such as the Brooks and Corey (1964) (BC) equation or the van Genuchten (1980) equation, to the average saturation versus capillary pressure data pairs using the method of least squares. However, the resulting parameter estimates depend upon the sample dimensions and experimental setup (Cheng et al., 2013).

If the distribution of liquids within the sample is unknown, then the capillary pressure–saturation function at any physical point in the sample, $S(\psi)$, is also unknown. As a result, hanging water column, pressure cell, and centrifuge experiments produce an average capillary pressure–saturation function for the sample, $<S>(\psi)$, rather than the point, $S(\psi)$, function. Parameters describing the $<S>(\psi)$ depend upon the sample/

Abbreviations: RMSE, Root mean square error; BC, Brooks and Corey; TDR, Time-domain reflectometry.

* Corresponding author.
E-mail addresses: clark.cropper@volstate.edu (S.C. Cropper), eperfect@utk.edu (E. Perfect), chulin.cheng@utrgv.edu (C.-L. Cheng), lmckay@utk.edu (L. McKay), mskang007@gmail.com (M. Kang).

http://dx.doi.org/10.1016/j.geoderma.2016.09.034
0016-7061/

cell height over which the averaging has been measured. Average <S>(ψ) functions can differ significantly from point S(ψ) functions (Cropper et al., 2011).

Liu and Dane (1995a) derived analytical expressions, based on height-averaging, that relate the point, S(ψ), function to the average function, <S>(ψ):

$$\psi = \langle\psi\rangle + z_n\frac{\rho_n}{\rho_w} - z_w + \left(1-\frac{\rho_n}{\rho_w}\right)z \tag{1a}$$

$$\langle S\rangle = \frac{1}{z_c}\int_0^{z_c} S(\psi)dz \tag{1b}$$

where ‹ψ› is the average capillary pressure head, <S> is the height averaged relative saturation, ψ is the point capillary pressure head, S is the point relative saturation (location dependent), z_n and z_w are the heights where the pressures of the non-wetting (i.e. air) and wetting (i.e. water) fluids are measured respectively, z is the height at a point, z_c is the cell height, and ρ_n and ρ_w are the densities of the non-wetting and wetting fluids respectively. Eq. (1a) and (1b) allows for the inverse determination of point functions from average functions obtained using experimental methods such as the hanging water column, pressure cell, or centrifuge.

Point water retention functions are more likely to have an obvious air entry value than average functions (Sakaki and Illangasekare, 2007; Cheng et al., 2013). Thus, parameterization using the BC equation, which has a pronounced break in slope at this value, is preferred over fitting the van Genuchten (1980) equation which is a continuous function. Liu and Dane (1995b) used Eq. (1a) and (1b) to inversely estimate point parameters for the BC equation from average pressure cell retention data. Jalbert et al. (1999) introduced a FORTRAN-based computer program (TrueCell) that automates this process. The TrueCell program is recommended for use in the standard reference on physical methods of soil analysis (Dane and Hopmans, 2002). However, Liu and Dane (1995a, 1995b) and Jalbert et al. (1999) never validated the TrueCell approach against actual measurements of point capillary pressure–saturation functions.

In contrast to methods based on measuring outflow, time domain reflectometry (TDR) and various digital imaging technologies allow the distribution of liquids to be measured within a sample as it is subjected to step changes in capillary pressure. Sakaki and Illangasekare (2007) measured point S(ψ) functions using TDR probes installed at the midpoint of sample height in nine columns of sandy materials. Imaging technologies such as gamma beam attenuation (Dane et al., 1992), magnetic resonance imaging (MRI) (Chen and Balcom, 2005), neutron radiography (Kang et al., 2014), and X-ray computed tomography (CT) (Bayer et al., 2004) have also been successfully employed to determine point capillary pressure–saturation curves for various porous media.

Despite the availability of appropriate measurement techniques, we are only aware of two previous studies that have validated the performance of the TrueCell program against independent point water retention data. Sakaki and Illangasekare (2007) and Kang et al. (2014) compared point BC parameters extracted from average saturation data using the TrueCell program with those obtained from actual point measurements of S(ψ). Both studies found reasonable agreement between the measured point BC parameters and the estimates from TrueCell. However, the samples investigated within each study, were all the same height. Given the inclusion of TrueCell in the standard text on physical methods of soil analysis, a more robust validation, with samples of varying heights, is warranted.

The objective of this paper is to test the hypothesis that TrueCell can be employed to predict point BC parameters based on measured average capillary pressure–saturation data collected over a wide range of sample heights. To facilitate the drainage process and reduce other sources of experimental variability we employ a single homogenous porous medium: Flint sand. Our comparison is achieved through the following steps:

(i) Measure average water retention in Flint sand columns of various heights using the hanging water column method;
(ii) Use TrueCell to extract point BC equation parameters from the observed average retention data;
(iii) Fit the BC equation to point capillary pressure-saturation functions measured on Flint sand by Kang et al. (2014) using neutron radiography;
(iv) Compare point BC parameters obtained from the point and average data sets and their predicted capillary pressure–saturation functions.

2. Materials and methods

2.1. Flint sand

Flint sand (Flint #13, U.S. Silica Company, Berkeley Springs, WV) was selected as the material for this study. It is a relatively coarse homogeneous porous medium, facilitating relatively short pressure equilibrium times over the range of column heights studied. Sand grain diameters for this material range from 0.11 to 0.60 mm with a median grain diameter of 0.56 mm. It is mainly composed of quartz (99.8%), has a particle density of 2.65×10^3 kg m^{-3}, and a saturated hydraulic conductivity of $1.66 \pm 0.32 \times 10^{-4}$ m s^{-1} (U.S. Silica Company, 2009).

2.2. Point function data and parameterization

Kang et al. (2014) employed neutron radiography combined with a hanging water column setup and quasi-equilibrium drainage technique to characterize the point drainage behavior of a 5.6 cm tall column of Flint sand. The method is based on measuring the transmitted intensity of neutrons through a sample. Neutrons are attenuated differently by water and mineral solids. Through calibration the spatial distribution of water is obtained by mapping the attenuation of neutrons transmitted through the sample. The capillary pressure–saturation behavior at any point within the sample can then be determined by observing changes in the volumetric water content (θ) during quasi-equilibrium drainage increments.

The Kang et al. (2014) data set comprised 1080 paired observations of volumetric water content and capillary pressure head, with capillary pressure heads ranging between 2.66 cm and 51.73 cm. The data pairs were measured at different locations (corresponding to the intersections of an 8 by 15 grid) within the column, and were originally analyzed as 120 separate point capillary pressure–saturation curves. In the present study, these data were converted to effective saturation versus capillary pressure head data pairs, and were analyzed as a single point function for the entire column. Effective saturation, $S_e = (\theta-\theta_r)/(\theta_s-\theta_r)$, was calculated using the observed saturated (θ_s) and residual (θ_r) volumetric water contents. The volumetric water content at saturation (0.391 m^3 m^{-3}) was determined by averaging the eight (maximum) volumetric water contents measured at the minimum imposed capillary pressure head (2.66 cm). The residual volumetric water content (0.018 m^3 m^{-3}) was determined by averaging the eight (minimum) volumetric water contents measured at the maximum imposed capillary pressure head (51.73 cm).

The resulting effective saturation–capillary pressure data set was parameterized with the BC equation by fitting all 1080 data pairs to produce a composite point water retention function for Flint sand. The BC equation was fitted in the following form:

$$S_e(\psi) = \left(\frac{\psi_a}{\psi}\right)^{\lambda} \{\psi > \psi_a\} \tag{2a}$$

$$S_e(\psi) = 1 \qquad \{\psi \le \psi_a\} \tag{2b}$$

where ψ_a is the air entry value and λ is the pore-size distribution index. Eq. (2a) and (2b) was fitted to the neutron radiography data using segmented nonlinear regression analysis (Marquardt method) in SAS 9.4 (SAS Institute Inc., 2012). The goodness of fit was assessed based on the root mean square error (RMSE).

2.3. Hanging water column experiments

The hanging water column setup (Fig. 1) consisted of clear 3/4-in. PVC pipe (inner diameter = 1.83 cm) connected with Tygon tubing via an outlet at its base to a burette filled with water. A pressure transducer (PX409USB, Omega®, Manchester, UK) was attached to the burette and set to record cumulative water outflow at regular time intervals ranging from 1 to 30 s. The bottom of the clear PVC pipe was covered with four layers of moist Whatman #4 filter paper to provide a phase barrier. The column was filled with water and any trapped air in the hanging water column setup was removed. Flint sand was incrementally added to the water in the column in ~4 cm layers and the column was tapped to minimize air entrapment until the sand column reached the desired height. Completed sand columns were fully saturated with water by raising the water level in the burette to a height equal to the top of the sand pack, or slightly higher, and allowed to equilibrate overnight prior to drainage.

At the beginning of each drainage experiment the water table was adjusted to the top of the sand pack, and the fully saturated sand column was clamped to a stationary stand. The sand column was drained stepwise by lowering the hanging water column setup on an adjustable stand. Pressure head steps were typically ~3 cm, but were increased up to ~15 cm if low water outflow indicated that residual saturation was being approached. After each step, and at intervals between steps, the water level in the hanging water column burette, the volume of water in the burette, and the transducer outflow reading were recorded and later used to construct the main drainage curve. A real-time graphic display of outflow reported by the pressure transducer was used to judge when quasi-equilibrium conditions had been reached for each increment. Data pairs of capillary pressure head and saturation were collected at each quasi-equilibrium step. Drainage continued in this manner for each column until air passed the phase barrier.

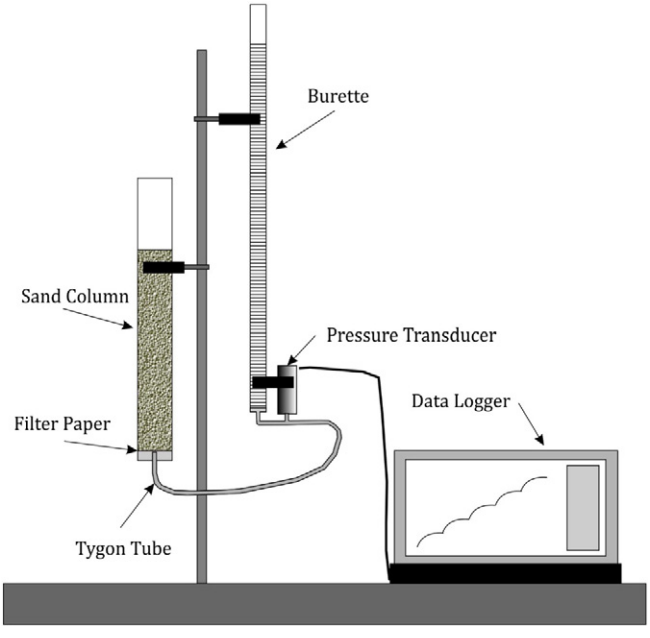

Fig. 1. Hanging water column laboratory setup showing sand column, burette, pressure transducer, and data logging computer.

After drainage was complete, the column sand was oven dried for 24 h at 105 °C and weighed for bulk density and porosity calculations. Bulk density was computed from the mass of oven dry sand/total volume of the packed sand column. The porosity was computed as 1 - bulk density/particle density.

A total of 11 Flint sand columns of different heights were prepared and drained using the hanging water column method described above. Additionally, unpublished data from one hanging water column experiment performed by Kang (personal communication) using the same Flint sand and the same experimental technique were included. Column heights for the 12 columns investigated are listed in Table 1.

2.4. Inverse estimation of point parameters

TrueCell (Jalbert et al., 1999) was used to inversely extract point BC parameters from the average water retention data observed during drainage of each column. TrueCell requires column configuration details including column height, z_c, the position where nonwetting fluid pressure was measured relative to the bottom of the column, z_n, the position where wetting fluid pressure was measured relative to the bottom of the column, z_w, and the densities of the non-wetting and wetting fluids. For all of the hanging water column experiments, the top of the column was used for the TrueCell corrections. As a result, $z_w = z_n = z_c$. Fluid densities for all columns were assumed to be 1.220 kg m^{-3} and 1000 kg m^{-3} for ρ_n (air) and ρ_w (water) respectively.

TrueCell was implemented in effective saturation mode, with two fitting parameters (ψ_a and λ), and two constants (θ_s and θ_r). The point estimates for ψ_a and λ produced by fitting the neutron radiography data of Kang et al. (2014) (see Section 2.2) were used as initial guesses for the two fitting parameters. The θ_s and θ_r parameters were fixed to the measured maximum and minimum volumetric water contents for each hanging water column experiment.

3. Results

Table 1 contains the measured bulk densities, and the maximum (θ_s) and minimum (θ_r) volumetric water contents for each packed sand column. The maximum water content is equal to the porosity. The mean column bulk density was 1721 kg m^{-3}, with a coefficient of variation (CV) of 3.71%. The mean θ_s was 0.350, with a CV of 6.99%. The mean θ_r was 0.042, with a CV of 24.12%. The CV for θ_r was much higher than the CV's for the other physical properties. This is because the mean value for θ_r (which is the denominator in the expression for CV) was very close to zero.

Table 1
Physical properties of the different columns of Flint sand.

Column height (run number)	Bulk density (kg m^{-3})	Saturated water content (m^3 m^{-3}) †	Residual water content (m^3 m^{-3})
4.3 cm (R0)	1740	0.344	0.040
14.4 cm (R7)	1780	0.327	0.046
19.7 cm (R10)	1780	0.327	0.021
23.8 cm (R5)	1680	0.367	0.056
24.5 cm (R1)	‡	‡	‡
24.9 cm (R11)	1750	0.339	0.054
25.1 cm (R2)	1620	0.389	0.048
29.5 cm (R3)	1650	0.377	0.039
37.0 cm (R4)	1630	0.385	0.049
43.3 cm (R8)	1780	0.327	0.036
48.5 cm (R6)	1740	0.343	0.041
55.0 cm (R9)	1780	0.329	0.032

† Equal to the computed porosity.
‡ Not measured.

Table 2
Range of capillary pressure head, number of equilibrium steps, total drainage time, and transducer interval for Flint sand hanging water column experiments.

Column height (run number)	Capillary pressure head range (cm)	Equilibrium steps	Total drainage time (h)	Transducer interval (s)
4.3 cm (R0)	0–41.7	16	5.0	1
14.4 cm (R7)	0–76.7	15	31.3	15
19.7 cm (R10)	0–59.6	16	74.6	30
23.8 cm (R5)†	0–41.9	9	93.2	1
24.5 cm (R1)†	0–43.1	12	5.1	1
24.9 cm (R11)	0–67.4	17	76.9	30
25.1 cm (R2)†	0–47.2	16	11.3	1
29.5 cm (R3)	0–85.2	25	32.0	1
37.0 cm (R4)	0–66.3	22	47.3	1
43.3 cm (R8)	0–116.6	19	293.7	30
48.5 cm (R6)	0–123.9	20	191.8	1
55.0 cm (R9)	0–108.7	20	301.2	30

† Incomplete drainage set.

Table 2 shows the number of capillary pressure head increments, the range of capillary pressure heads, and total drainage times for each column. Equilibrium steps above the air-entry pressure were easy to distinguish using the graphic display of water outflow. Fig. 2 shows the pattern of outflow equilibrium steps for three selected columns.

Air passed the phase barrier prior to reaching residual saturation during drainage of three columns leaving 9 water retention data sets with sand column heights ranging from 4.3 cm to 55.0 cm (Table 2). The 9 complete data sets contain at a minimum 15, and as many as 25 equilibrium steps. Drainage durations ranged from 5 h (4.3 cm column) to ~12.5 days (55.0 cm column).

The average capillary pressure–saturation data sets collected during drainage of each column are shown in Fig. 3. These data sets were processed in TrueCell (Jalbert et al., 1999) to extract point BC parameter estimates for each column. The resulting point BC parameter estimates and root mean square error (RMSE) statistics are shown in Table 3, which also includes the point parameter estimates obtained by fitting the BC equation to the neutron radiography data set of Kang et al. (2014). The capillary pressure–saturation functions predicted by the point BC parameters for the different columns are plotted in Fig. 3 for comparison with the measured average capillary pressure–saturation data sets. It can be seen that there are marked differences in the shapes of the average and point functions, and these differences become more pronounced as the column height increases.

Average values of the predicted point parameters in Table 3 were 16.253 cm and 8.492 for ψ_a and λ, respectively, as compared to 16.928 cm and 5.668 for ψ_a and λ, respectively, from the neutron imaging experiment. One sample t-tests indicated that there were no significant differences (at $p < 0.05$) between the mean parameter values and the corresponding neutron radiographic estimates.

Fig. 4 compares the TrueCell point BC parameter estimates to the point BC parameters fitted to the neutron imaging data of Kang et al. (2014). The neutron imaging parameters are shown as dashes with 95% confidence intervals as gray bars. The 95% confidence intervals for the air-entry (ψ_a) parameter had a very small range (± 0.12 cm). Only the 48.5 cm column had an estimate of ψ_a that fell within the 95% confidence limits. The maximum deviation for ψ_a was $+3.43$ cm for the 14.4 cm column. Air entry estimates for all other columns underpredicted the observed air entry value. The 95% confidence range for the pore size distribution index, λ, was also small (± 0.51). The parameter estimate of λ for one column, 48.5 cm, fell within this range. The maximum deviation for λ was $+25.78$ for the 37.0 cm column, which was much higher than all the other deviations.

A correlation matrix was computed for the following variables: bulk density, θ_s θ_r, ψ_a, λ, and column height. Statistical significance was

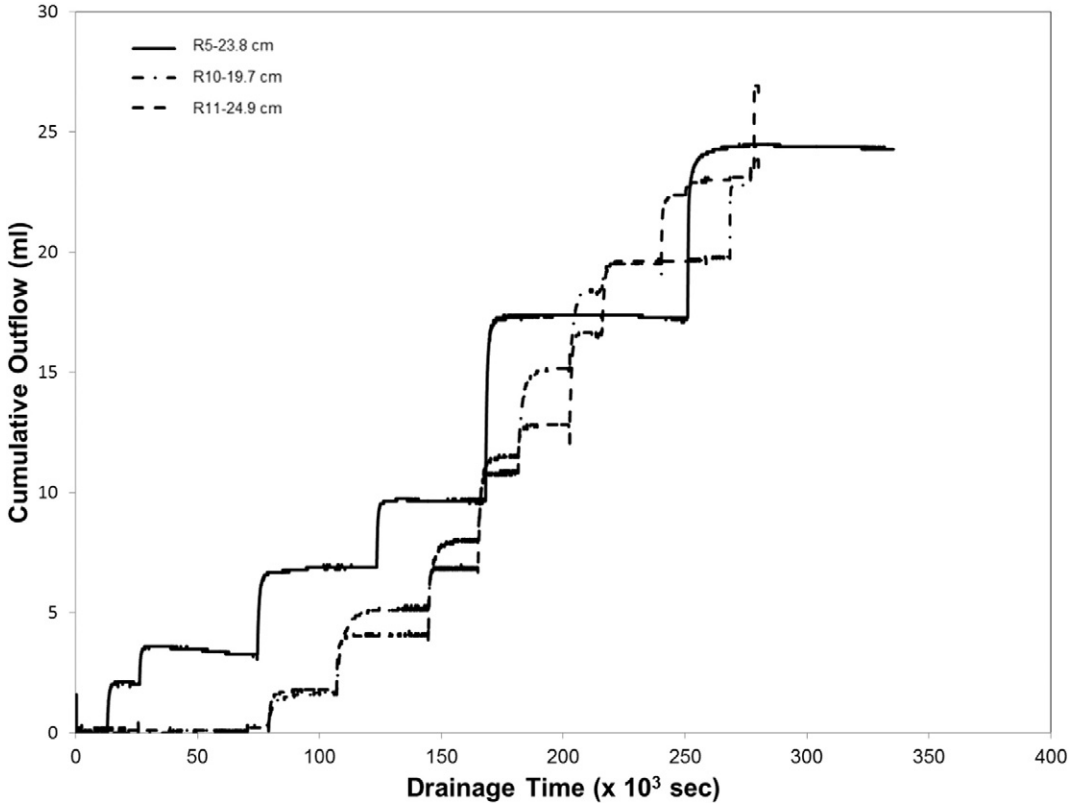

Fig. 2. Cumulative water outflow through time for the 23.8 cm, 19.7 cm, and 24.9 cm Flint sand hanging water column drainage experiments.

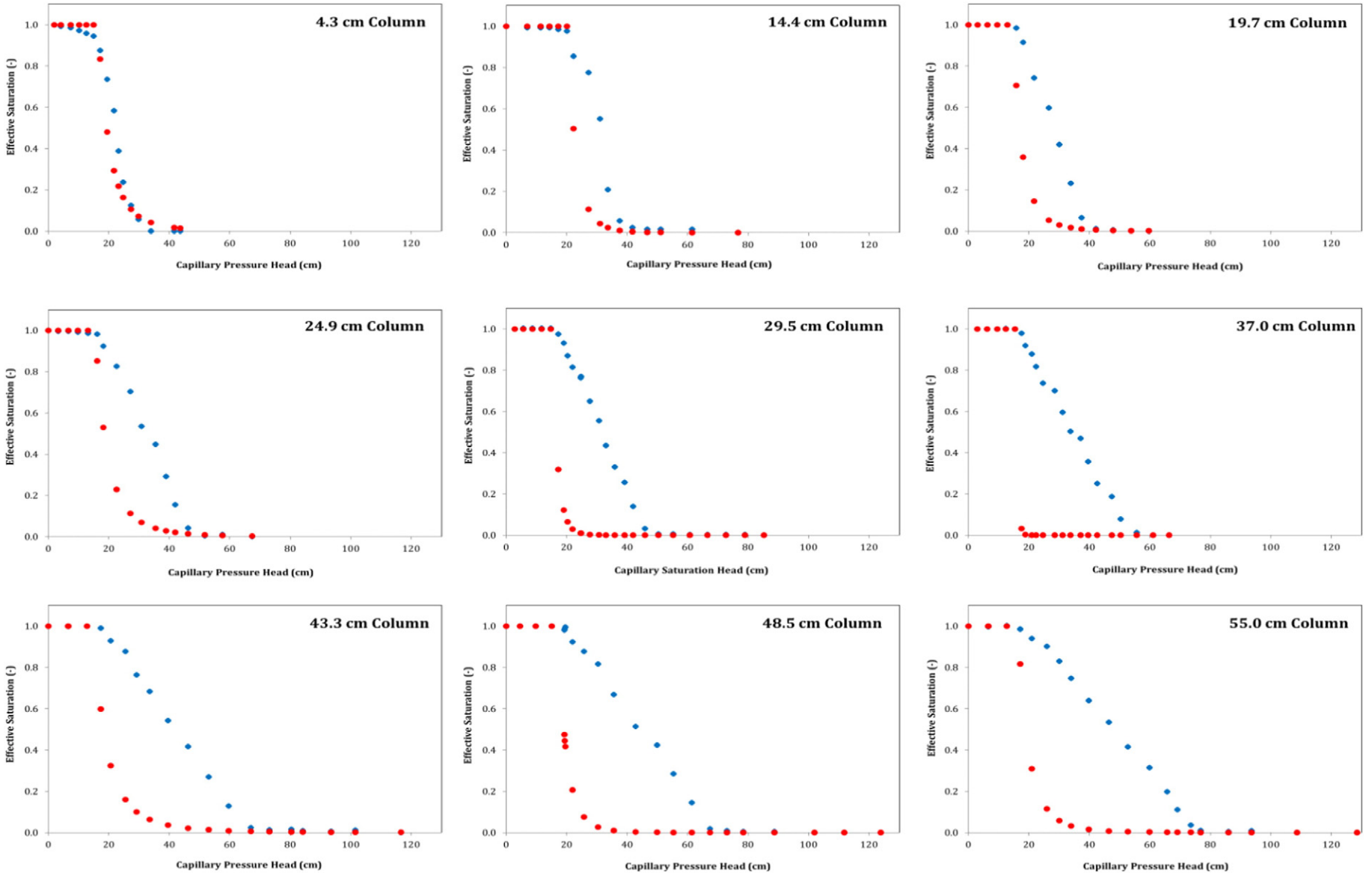

Fig. 3. Measured average capillary pressure–effective saturation data pairs (blue) and predicted point values (red) from TrueCell (Jalbert et al., 1999) for the nine column heights of Flint sand.

Table 3
Summary of Brooks and Corey (1964) equation point parameters estimated by TrueCell (Jalbert et al., 1999) from average capillary pressure-saturation data for nine columns of Flint sand. The measured neutron imaging point BC parameters are also included for comparison.

Column height (run number)	ψ_a (cm)	λ	RMSE
4.3 cm (R0)	16.5	4.4	4.96×10^{-2}
14.4 cm (R7)	20.4	7.5	4.52×10^{-2}
19.7 cm (R10)	14.7	5.0	1.94×10^{-2}
24.9 cm (R11)	15.5	3.9	2.65×10^{-2}
29.5 cm (R3)	15.3	9.7	1.33×10^{-2}
37.0 cm (R4)	15.7	31.4	1.85×10^{-2}
43.3 cm (R8)	14.9	3.4	1.10×10^{-2}
48.5 cm (R6)	17.1	6.3	1.35×10^{-2}
55.0 cm (R9)	16.4	4.7	1.16×10^{-2}
Neutron imaging	16.9	5.7	4.33×10^{-2}

assessed the $p < 0.05$ probability level. There were no significant correlations between column height and any of the physical/hydraulic parameters investigated. The only significant correlations were between bulk density and λ, and θ_s and λ ($r = -0.789$ and $r = 0.787$, respectively). These correlations indicate that the steepness of the capillary pressure–saturation curve (as indicated by increasing λ) increased with decreasing bulk density and increasing porosity/maximum water content. They appear to be driven by the two columns with the highest bulk density/lowest porosity values (i.e., R3 and R4), which also had the highest λ values (Tables 1 and 3).

4. Discussion and conclusions

The objective of this paper was to test the hypothesis that TrueCell can predict point hydraulic functions from measured average capillary pressure-effective saturation retention data. To test this hypothesis, measured average retention data sets for 9 different column heights were processed in TrueCell to produce 9 point BC parameter sets.

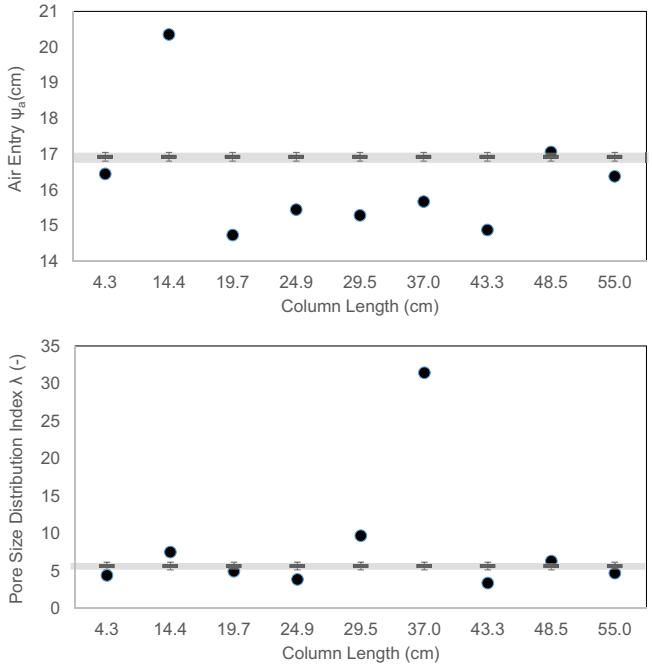

Fig. 4. Relationship between TrueCell (Jalbert et al., 1999) estimates of air entry (ψ_a) parameters and pore size distribution index (λ) parameters shown as circles, and parameter values determined by neutron imaging. Neutron imaging values are shown as dashes with 95% confidence intervals as error bars (gray).

These values were compared to point BC function parameters determined by neutron radiographic imaging of a hanging water column experiment.

One sample t-tests indicated no significant differences (at $p < 0.05$) between the mean values of the 9 inverse estimates of ψ_a and λ from TrueCell and the corresponding neutron imaging estimates. However, the individual TrueCell predictions produced quite variable results compared to the measured point parameter set from neutron imaging (Fig. 4). Relatively few parameter estimates fell within the 95% confidence intervals of the neutron imaging estimates, and some deviations were quite large. This variability did not seem to be related to column height, but rather to subtle differences in column packing.

With inverse modeling it is possible to achieve approximately the same fit to a function with different sets of parameter estimates. To determine if this was the case in this study, point effective saturations predicted using the parameter sets from TrueCell were compared with those predicted using the observed neutron imaging parameter set. Fig. 5 shows the predicted functions plotted against the observed functions for all 9 column heights. Good correspondences between the effective saturations plot close to the (dashed) one-to-one line. The three longest columns (43.3, 48.5, and 55 cm) show very good correspondence. Two other columns (4.3 and 24.9 cm) show reasonable correspondence, but the remaining four columns show little to no correspondence. Based on these results it is clear that the relationship between point functions extracted from average capillary pressure–saturation data using TrueCell and independently measured point functions can be highly variable.

A previous study by Sakaki and Illangasekare (2007) using TrueCell found reasonable agreement between TrueCell predicted BC parameters and independently determined values for 9 different materials using the same column height. Although there was under-prediction of the λ parameter compared to the observed values, the predicted saturation functions were generally good. Kang et al. (2014) obtained multiple sets of point BC parameters for a single column of Flint sand using neutron radiography. A single BC point water retention function was constructed using the median values of these parameter estimates. This curve corresponded closely with the single point BC function inversely extracted from the average water retention data using TrueCell.

Possible explanations for the apparent contradiction between the results of previous studies and those of the current study might be: (i) variability in the packing of multiple columns of the same material, and (ii) unrepresentative observed point parameters. We measured average drainage behavior for the same material packed in multiple columns with different heights, whereas Sakaki and Illangasekare (2007) measured different materials with the same column height, while Kang et al. (2014) only compared results for a single column. The variability encountered in our study does not appear to be related to column height. Instead, subtle differences in packing between columns may have influenced the estimates of point parameters extracted by TrueCell for the same material. Additionally, it is worth noting that Sakaki and Illangasekare (2007) observed point drainage behavior on multiple columns, whereas we relied on results from only one column.

This study has produced some support for inverse modeling with TrueCell, in that the approach was shown to be reliable on average. However, it often failed in predicting specific BC parameters for individual columns. Although TrueCell successfully predicted point effective saturation functions for some columns, the overall variability observed in the predictions suggests that this computational procedure should be used with caution.

In future investigations of a similar nature, it may be useful to independently determine point BC parameters on multiple columns (instead of on one as was done in the present study) for comparison with the parameters extracted from average retention functions using TrueCell. This investigation also suggests that further research on the nature of the relationship between variations among individual parameters within a parameter set and the resulting predicted function may be valuable.

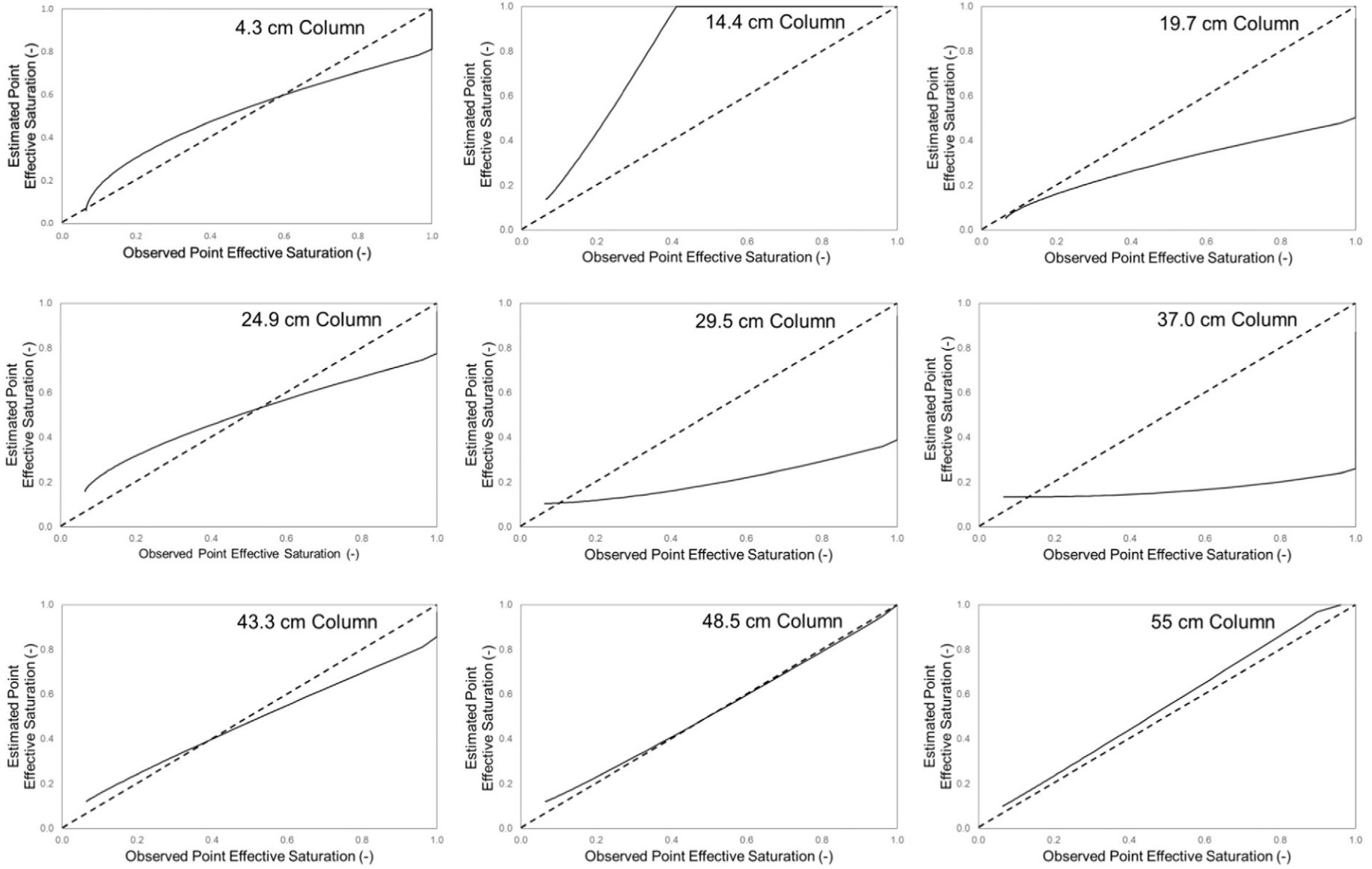

Fig. 5. Estimated point effective saturations determined using parameter sets from TrueCell for nine column heights of Flint sand compared with observed point effective saturations determined from the parameter set obtained by neutron radiography. The dashed line indicates one to one correspondence.

References

Bayer, A., Vogel, H.-J., Roth, K., 2004. Direct measurement of the soil water retention curve using X-ray absorption. Hydrol. Earth Syst. Sci. 8 (1), 2–7.

Brooks, R.H., Corey, A.T., 1964. Hydraulic Properties of Porous Media. Hydrology Papers 3. Colorado State Univ., Fort Collins.

Chen, Q., Balcom, B.J., 2005. Measurement of rock-core capillary pressure curves using a single-speed centrifuge and one-dimensional magnetic-resonance imaging. J. Chem. Phys. 122 (21), 214720–214727.

Cheng, C.-L., Perfect, E., Mills, R.T., 2013. Forward prediction of height-averaged capillary pressure–saturation parameters using the BC-vG Upscaler. Vadose Zone J. 12 (3).

Cropper, S.C., Perfect, E., van den Berg, E.H., Mayes, M.A., 2011. Comparison of average and point capillary pressure–saturation functions determined by steady-state centrifugation. Soil Sci. Soc. Am. J. 75 (1), 17–25.

Dane, J.H., Hopmans, J.W., 2002. Computational Corrections. In: Dane, J.H., Topp, C.G. (Eds.), Methods of Soil Analysis: Part 4 Physical Methods. Soil Science Society of America, Madison, WI, pp. 714–717 (Chapter 3.3.2.10).

Dane, J.H., Oostrom, M., Missildine, B.C., 1992. An improved method for the determination of capillary pressure-saturation curves involving TCE, water and air. J. Contam. Hydrol. 11, 69–81.

Jalbert, M., Dane, J.H., Liu, J.H., 1999. TrueCell: Physical Point Brooks–Corey Parameters Using Pressure Cell Data. Users Guide for Version 1.2. Special Report. Department of Agronomy and Soils, Auburn Univ., Auburn, AL.

Kang, M., Perfect, E., Cheng, C.L., Bilheux, H.Z., Lee, J., Horita, J., Warren, J.M., 2014. Multiple pixel-scale soil water retention curves quantified by neutron radiography. Adv. Water Resour. 65, 1–8.

Liu, H.H., Dane, J.H., 1995a. Improved computational procedure for retention relations of immiscible fluids using pressure cells. Soil Sci. Soc. Am. J. 59, 1520–1524.

Liu, H.H., Dane, J.H., 1995b. Computation of the Brooks–Corey Parameters at a Physical Point Based on Pressure Cell Data. Special Report, Department of Agronomy and Soils. Auburn Univ, Auburn, AL.

Sakaki, T., Illangasekare, T.H., 2007. Comparison of height-averaged and point measured capillary pressure–saturation relations for sands using a modified Tempe cell. Water Resour. Res. 43:W12502. http://dx.doi.org/10.1029/2006WR005814.

SAS Institute Inc, 2012. SAS/STAT version 9.4 Cary, NC, USA. Comput. Softw.

U.S. Silica Company, 2009. Product Data Sheet: Whole Grain Silica. Berkeley Springs, WV.

van Genuchten, M.T., 1980. A closed-form equation for predicting the hydraulic conductivity of unsaturated soils. Soil Sci. Soc. Am. J. 44, 892–898.